Ab-Initio Study of Initial Atmospheric Oxidation Reactions of C_3 and C_4 Alkanes

ISIDORO GARCÍA-CRUZ,[1] M. E. RUIZ-SANTOYO[1]
J. RAÚL ALVAREZ-IDABOY,[2] ANNIK VIVIER-BUNGE[3]

[1] *Gerencia de Ciencias del Ambiente, Instituto Mexicano del Petróleo, 07730 México, D.F., México*
[2] *Laboratorio de Química Computacional y Teórica, Facultad de Química, Universidad de La Habana, Habana 10400, Cuba*
[3] *Departamento de Química, Universidad Autónoma Metropolitana, Iztapalapa, 09340 México, D.F., México*

Received 16 August 1998; accepted 8 January 1999

ABSTRACT: Second-order, Møller–Plesset (MP2)-unrestricted Hartree–Fock calculations with full geometry optimization in the 6-31G(*d*, *p*) basis set were carried out to study the initial atmospheric oxidation reactions of alkanes. All structures in the initial hydrogen abstraction reaction by an OH radical and the subsequent addition of molecular oxygen to the alkyl radical were characterized for alkanes with three and four carbon atoms. The reaction paths for the formation of the peroxyl radicals were obtained and discussed in the light of similarities along series involving primary, secondary, and tertiary hydrogens. A 0.999 correlation was found between the height of our barriers for the OH abstraction of a primary hydrogen atom from alkanes containing one to four carbon atoms and the optimally estimated activation energies for this reaction recently presented. From the slope and the intersection at zero activation energy an equation was obtained that yields scaled values of the activation energies to account for the tunnel effect and for the error due to the basis set and the method employed. We present new results for the abstraction of the less favored primary hydrogens in propane, butane, and isobutane, which should be important at high temperatures. Negative net activation energies were obtained for the addition of molecular oxygen to all the alkyl radicals formed in the first reaction. The structure of the peroxyl radicals is discussed; and very good correlations are observed for similar compounds, regardless of the length of the carbon chain. A revision of some experimental values is suggested. Single point density functional calculations at the MP2 geometries were also performed with the B3LYP functional for comparison. The observed trends are exactly the same

Correspondence to: A. Vivier-Bunge; e-mail: annik@xanum.uam.mx

CCC 0192-8651 / 99 / 080845-12

for the two methods. © 1999 John Wiley & Sons, Inc. J Comput Chem 20: 845–856, 1999

Keywords: hydroxyl radical; alkanes; atmospheric reactions; hydrogen abstraction; alkyl peroxyls; activation energies

Introduction

The initial reaction of alkanes in the troposphere involves, almost exclusively, the OH· radical via the abstraction of a hydrogen atom to form water and an alkyl radical[1]:

$$RH + OH\cdot \rightarrow R\cdot + H_2O. \quad (1)$$

Hydrocarbon radicals formed in (1) react immediately with molecular oxygen to form peroxyls,

$$R\cdot + O_2 \rightarrow ROO\cdot, \quad (2)$$

which in turn combine with nitric oxide according to the following equations:

$$ROO\cdot + NO \rightarrow R\cdot O + NO_2 \quad (3)$$

and

$$ROO\cdot + NO \rightarrow RONO_2. \quad (4)$$

Reactions (3) and (4) are responsible for altering the ratio NO_2/NO, but it is normally accepted[1] that reactions (1) and (2) are the ones that determine the ozone forming capability of alkanes.

The importance of understanding these reactions and the need to control the formation of ozone to achieve ozone air quality standards is well recognized. Methane is, by far, the most abundant hydrocarbon in urban atmospheres; and it has recently been discovered[2] that propane and butane are unusually abundant in Mexico City's air, due mainly to losses from liquid gas tanks used in domestic chores. Although alkanes are not very reactive species, they are thought[1] to constitute the dominant OH sink; thus, their reactions are important for the chemistry of the troposphere.

A vast amount of experimental kinetic data for the reaction of volatile organic compounds with the OH· radical are available. Atkinson et al.[3,4] reported rate constant values for the hydrogen abstraction from alkanes with OH·, as well as expressions of the form $k = CT^n e^{-D/T}$ to fit the experimental data. Recently, Donahue et al.[5] assessed the accuracy of the measurement of the rate constants for 10 of these reactions involving alkanes with two to eight carbon atoms, and they report corresponding estimated Arrhenius parameters that fit data over a wide temperature range. These rate constants and activation energies, however, do not distinguish between the different types of hydrogen atoms involved and can be assumed to refer to a hydrogen atom abstracted from the more substituted carbon atom.

Theoretical studies based on experimental data were also performed[6–10] for reaction (1) to design a model for OH-alkane reactions for extrapolating from measured rate coefficients to unmeasured ones. Quantum chemical studies focusing on the molecular aspects of the kinetics of this reaction at low temperatures for the simplest alkanes (methane,[11] ethane,[12] and propane[13]) were carried out. Because Arrhenius plots of experimental data for reaction (1) characteristically present considerable curvature,[4] it is expected that tunneling plays an important role at temperatures below 700 K. In fact, Melissas and Truhlar estimated[11] on the basis of theoretical calculations that more than half the reactive events in the hydrogen abstraction from methane in the 300–500 K range occur by tunneling. Gonzalez–Lafont et al.[14] developed a hierarchy of approximations for quantized variational transition state theory and semiclassical tunneling calculations to predict reaction rate constants from a limited set of information about the potential energy surface. They tested their method first on the methane + OH· reaction, which is the prototype for H abstraction reactions from hydrocarbons. Truong and Truhlar[15] performed a sequence of calculations with methods of increasing precision up to second-order Møller–Plesset (MP2) with a variety of basis sets, and they estimated the rate constant of reaction (1) for methane in the temperature range from 200 to 2000 K. Melissas and Truhlar[12] applied the same method to reaction (1) for ethane and, more recently, accurate theoretical calculations were performed on the mechanism of the hydrogen abstraction from ethane and chloroethane.[16] Garcia–Cruz et al.[17] used MP2 calculations to obtain the energies and structures of the species involved in the OH abstraction of primary, secondary and tertiary hydrogens from propane, butane, and isobutane. Hu et al.[13] optimized the geometries at the MP2 level, scaled according to the scaling all correlation method

(SAC),[18] and they used variational transition state theory with semiclassical tunneling to calculate rate constants for the OH-propane reaction for propane and five different isotopic analogues of propane for abstraction of both primary and secondary hydrogen atoms.

The experimental k values of reaction (2) are given in Table I as reported in ref. 3: they are the high-pressure rate constants k_∞ at room temperature. No fits to Arrhenius type equations are available. However, the reaction of ethane with O_2 was studied experimentally by Dobis and Benson[19] at very low pressures and in the 243–368 K temperature range. Under these conditions, the radical oxidation is suggested to occur via a vibrationally excited ethylperoxy radical that cannot be collisionally stabilized and that isomerizes to 2-hydroxyperoxyethyl radical, finally producing ethylene. The authors obtained the activation energy for the C_2H_5 consumption that should be the same as the activation energy of reaction (2).

Reaction (2) is characterized by having a rate that decreases with increasing temperature. Singleton and Cvetanovic[20] explained the occurrence of these negative activation energies in apparently elementary, high pressure limit gas phase reactions as being due to the formation of a loosely bound prereactive complex that is formed in a reversible reaction without activation energy, followed by a second reaction whose transition state energy is lower than the energy of the separated reactants and is irreversible. For reaction (2) one would have

$$R\cdot + O_2 \rightleftharpoons R\cdots O_2 \rightarrow RO_2. \qquad (5)$$

TABLE I.
Recommended High Pressure Rate Constants k_∞ for R· + O_2 Reactions at Room Temperature.[3]

R·	$10^{12} \times k_\infty$ (cm^3 molecule^{-1} s^{-1})
Primary	
Methyl	1.8
Ethyl	7.8
1-Propyl	8.0
1-Butyl	7.5
2-Methyl-1-propyl	2.9
Secondary	
2-Propyl	11.0
2-Butyl	16.6
Tertiary	
2-Methyl-2-propyl	23.4

The alkyl radicals are grouped according to the kind of carbon atom to which the O_2 is attached.

If k_1 and k_{-1} are the rate constants for the first step and k_2 corresponds to the second step, a steady-state analysis leads to a rate constant for the overall reaction that can be written as

$$k = \frac{k_1 k_2}{k_{-1} + k_2}. \qquad (6)$$

Even though the energy barrier for k_{-1} is about the same size as that for k_2,[21] the entropy change is much larger in the reverse reaction than in the formation of the products. Thus, one can expect that k_{-1} will be considerably larger than k_2. With this assumption, first considered in ref. 20, one obtains

$$k = \frac{k_2 k_2}{k_{-1}} = \left(\frac{A_1 A_2}{A_{-1}}\right) e^{-(E_1 + E_2 - E_{-1})/RT}. \qquad (7)$$

Because E_1 is zero, the net activation energy for the overall reaction is

$$E_a = E_2 - E_{-1} = (E_{TS} - E_{PR}) - (E_{reactants} - E_{PR}) = E_{TS} - E_{reactants}, \qquad (8)$$

where TS is the transition state and PR is the prereactive complex. Thus, the final expression for E_a turns out to be the usual expression for the calculation of any activation energy, regardless of the energy of the prereactive complex. The fact that a preequilibrium does not affect the kinetics is very well known.

The existence of the prereactive complexes was recently verified by *ab initio* quantum chemistry calculations for the OH addition to propene.[21] The mechanism proposed in ref. 20 was tested in our group[22] on the addition reaction of OH to a series of substituted ethylenes, and we found that it explains the experimental results.

The heats of formation of selected peroxyl radicals are given in Lightfoot et al.[23] On the theoretical side, methane and ethane peroxyls were the subject of several calculations.[23] The CH_3O_2 radical was studied in both the ground and low lying excited states by Jafri and Phillips[24] using the GVB-CI method. Quelch et al.[25] obtained optimized geometries for several conformers of the ethylperoxy radical and discussed their energies and interconversions in view of studying the mechanism of the $C_2H_5 + O_2$ reaction at high temperatures.[26] Boyd et al.[27] performed MP2/6-31G** calculations on 27 C_2 and C_3 peroxyls with a geometry optimization at the Hartree–Fock (HF) level to study the structures and properties of peroxyl radicals. Recently, Ignatyev et al.[28] studied

the mechanism of the $C_2H_5 + O_2$ reaction at high temperatures using density functional theory.

In this work, we studied reactions (1) and (2) for the abstraction of an H atom from small alkanes with up to four carbon atoms. In addition to performing the geometry optimizations with the MP2/6-31G** method, single point density functional calculations were made on the MP2 geometries using the B3LYP functional.[29] We report new results for the structure and energetics of the reactants, products, and transition state of reactions (1) and (2) for propane, butane, and isobutane; for channels involving the abstraction of either a primary, secondary, or tertiary H atom; and the addition of O_2 to the corresponding radical. Trends and correlations are discussed. An empirical method is proposed to scale the energy barrier to account for the tunnel effect, as well as for the errors due to the basis set and to the limited treatment of the correlation energy. Activation energies for reaction (2) are calculated according to eq. (8) and negative values are obtained and correlated with the rate constants in Table I. A revision of some experimental values is suggested. The structures and charges and spin densities of the peroxyl radicals are discussed.

Computational Methodology

Electronic structure calculations were performed with the system of programs Gaussian 94 (G94).[30] Restricted HF theory (RHF) is used for closed shell systems and unrestricted HF theory (UHF) for open shell systems (radicals). The correlation energy corrections are introduced with MP perturbation theory up to second order and results from spin projected calculations are used (PMP2 and PUMP2).

All geometries are fully optimized at the MP2/6-31G** level, and the character of the transition state is confirmed by a frequency calculation performed at the same level and presenting an imaginary frequency in the 453–2061 cm^{-1} range. Energies are corrected for the zero point vibrational energy and thermal terms are added for comparison with room temperature data.

Density functional B3LYP/6-31G** energy results are also obtained at the MP2 geometries.

Results

Our present study investigates the reaction paths for two consecutive reactions [reactions (1) and (2)] for propane, butane, and isobutane. Some features of the corresponding reactions for methane and ethane were recalculated for comparison. Reactants, transition states [TS1 and TS2 for reactions (1) and (2), respectively], and products were considered. The total PMP2 energies of the MP2/6-31G** optimized geometries are given in Table II, together with the zero point vibrational corrections and thermal corrections to the energy calculated at the same level. Also given in this table are the MP2 $\langle S^2 \rangle$ values before and after projection of higher spin states and the imaginary frequencies characterizing the transitions states. It is seen that for reaction (1), contamination by higher spin states is never very important. When the O_2 ground state is involved, however, the coupling between a doublet radical and the triplet molecular oxygen at large distances (in particular, for TS2) yields, as expected, a large contribution from quartet states, so that the $\langle S^2 \rangle$ value before projection is much too large (≈ 1.5). After projection, the $\langle S^2 \rangle$ for TS2 is 0.83. For all the stable radicals, spin contamination is negligible.

When the B3LYP method is employed, the $\langle S^2 \rangle$ values for reaction (2) are also nonnegligible. At the TS2 transition states, $\langle S^2 \rangle$ is about 0.93 and 0.752 before and after projection, respectively.

OH-ALKANE HYDROGEN ABSTRACTION REACTION

In the hydrogen abstraction reaction (1), the reaction coordinate is essentially the distance C···H between the H atom that is being abstracted and the C atom to which it is originally attached. The optimized geometry of the transition state (TS1) for the abstraction of a primary hydrogen atom from butane, calculated at the MP2/6-31G** level, is represented in Figure 1a where we indicate the main angles and distances. The corresponding values for propane and isobutane are found to be very similar with differences of only about 0.003 Å in bond lengths and of 0.1° in bond angles. The TS1 transition states are characterized by the following general properties:

1. They are closer to the reactants than to the products: C···H distances are smaller than H···O distances, meaning that they occur at the beginning of the reaction when the OH· radical is still somewhat far apart. This result is in agreement with the Hammond postulate, according to which transition states of exothermic reactions should be more reactantlike than productlike.

TABLE II.
PMP2 Total Energies (hartrees), Zero Point Vibrational Energy Corrections (ZPVE), Thermal Energies (TE), $\langle S^2 \rangle$ Values before and after Projection, and Imaginary Frequencies (ν_i) at Transition States.

System	PMP2 / 6-31G**	ZPVE	TE	S^2		ν_i
				Before	After	(cm^{-1})
OH	−75.533571	0.008753	0.011113	0.755	0.750	
H_2O	−76.219788	0.021879	0.024714	0.0	0.0	
O_2	−149.955766	0.003211	0.005579	2.0	2.0	
RH						
Propane	−118.725385	0.107094	0.111524	0.0	0.0	
Butane	−157.907453	0.136492	0.142158	0.0	0.0	
Isobutane	−157.910074	0.136057	0.141617	0.0	0.0	
TS1						
Propane-*p*	−194.248608	0.113254	0.119709	0.779	0.750	−1730
Propane-*s*	−194.249914	0.112822	0.119726	0.777	0.750	−1467
Butane-*p*	−233.430798	0.142208	0.150341	0.779	0.750	−1760
Butane-*s*	−233.433217	0.142614	0.150542	0.777	0.750	−1421
Isobutane-*p*	−233.433382	0.142160	0.149864	0.779	0.750	−1731
Isobutane-*t*	−233.437124	0.141798	0.150043	0.776	0.750	−1092
R						
Propane-*p*	−118.059025	0.090945	0.095202	0.763	0.750	
Propane-*s*	−118.063891	0.091668	0.09661	0.763	0.750	
Butane-*p*	−157.241358	0.120962	0.12698	0.762	0.750	
Butane-*s*	−157.245399	0.12227	0.127353	0.749	0.750	
Isobutane-*p*	−157.243199	0.120702	0.126596	0.762	0.750	
Isobutane-*t*	−157.251674	0.12113	0.127270	0.763	0.750	
TS2						
Propane-*p*	−268.020834	0.099631	0.106026	1.495	0.817	−791
Propane-*s*	−268.02875	0.099297	0.105943	1.501	0.826	−633
Butane-*p*	−307.203242	0.129019	0.136682	1.507	0.827	−639
Butane-*s*	−307.210876	0.128629	0.136620	1.532	0.835	−556
Isobutane-*p*	−307.204525	0.128684	0.136363	1.501	0.827	−637
Isobutane-*t*	−307.219523	0.127892	0.137178	1.535	0.836	−571
ROO						
Propane-*p*	−268.054468	0.103772	0.109778	0.761	0.750	
Propane-*s*	−268.061565	0.10323	0.109213	0.761	0.750	
Butane-*p*	−307.246511	0.133142	0.140523	0.761	0.750	
Butane-*s*	−307.24417	0.132639	0.139920	0.761	0.750	
Isobutane-*p*	−307.239039	0.132658	0.139967	0.761	0.750	
Isobutane-*t*	−307.251754	0.131619	0.138898	0.761	0.750	

The letter following the name of the alkanes refers to the type of hydrogen that is abstracted (i.e., primary, secondary, or tertiary). RH is the alkane; R is the alkyl radical, ROO is the peroxy radical; TS1 and TS2 stand for the transition states of reactions (1) and (2), respectively.

2. The C···H···O distance is, in all cases, approximately equal to 2.5 Å, which is characteristic of a hydrogen bonded bridge.[31]
3. The C···H···O angle is always close to 169° and curved in the same direction (i.e., the H of the OH· radical is in a cis position to the C atom).
4. The OH radical inserts preferentially in a gauche position with respect to the carbon chain. For propane, Hu et al.[13] also noted that the trans primary site transition state is less stable.

The optimized geometry of the TS1 transition state for a secondary hydrogen abstraction from butane is represented in Figure 1b. The main angles and distances are indicated on the figure, and corresponding values for propane are indicated in parentheses. The TS1 transition state for the hydro-

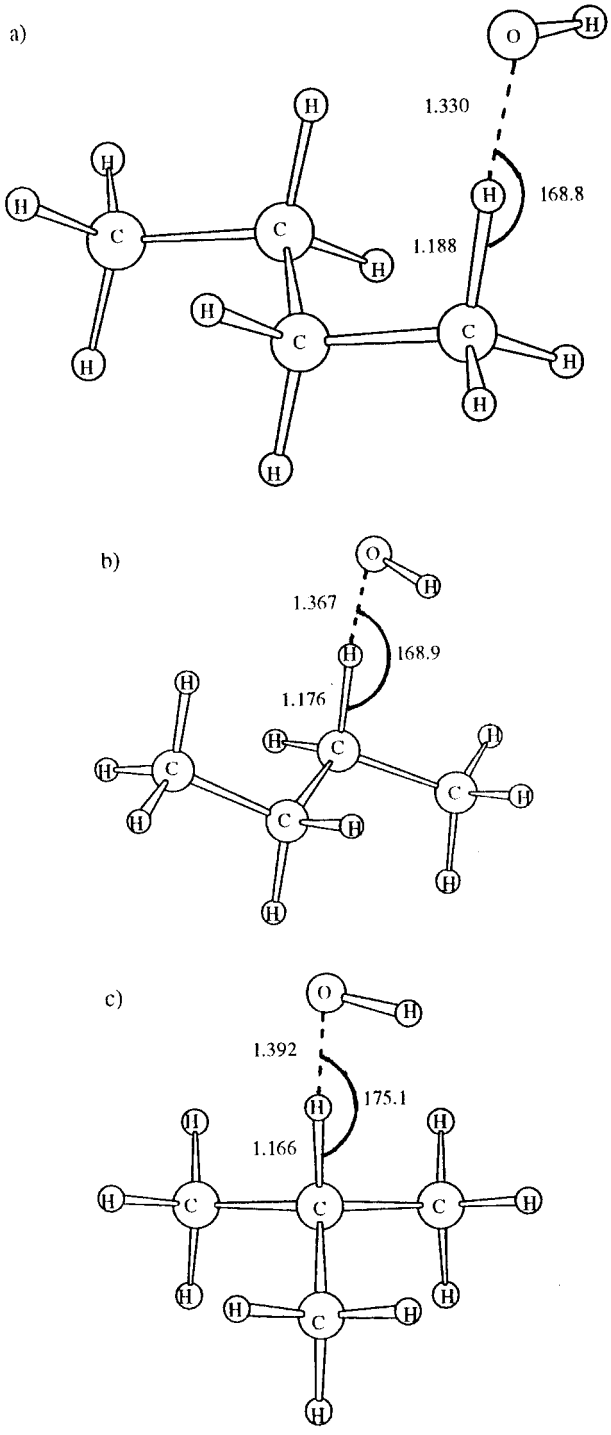

FIGURE 1. Optimized geometries of the transition states (TS1) for the OH-alkane hydrogen abstraction reaction. The TS1 for the abstraction of (a) a primary and (b) a secondary hydrogen atom from butane is shown. (c) The TS1 for a tertiary hydrogen from isobutane is represented.

gen abstraction of a tertiary hydrogen is represented in Figure 1c for isobutane.

There are obvious similarities among the properties of transition states involving the same kind of hydrogen atom (primary, secondary, or tertiary). Thus, for primary hydrogens, C···H values always lie at about 1.19 Å and H···O values at 1.33 Å; imaginary frequencies appear at 1730 cm^{-1}; charges are −0.49, −0.35, and +0.25 for the O, C, and H atoms involved in the bond, respectively, and spin densities are 0.72, 0.40, and −0.09 for those same atoms. For reactions abstracting secondary hydrogen atoms, we find that the C···H distance is smaller and the O···H distance is larger, which is in agreement with the well-known fact that secondary hydrogens are more reactive, so that the transition state is positioned earlier at the entrance of the reaction channel. Also, imaginary frequencies are smaller, implying less curvature of the potential energy curve at the transition state. The separation of charges is smaller, and the spin density is more localized on the oxygen atom. For the tertiary hydrogen, the same tendencies are observed, only more pronounced: the C···H distance is still smaller, the O···H distance is larger, the imaginary frequency is smaller, the charge separation is less pronounced, and the spin density on the oxygen atom continues to increase.

The optimized geometries for the C_3 and C_4 alkyl radicals are shown in Figure 2. The geometries of the favored conformers were thoroughly investigated to make sure that the observed minima were in fact absolute minima. In particular, in the case of the *n*-butyl radical, the potential energy curve for the torsion of the methyl group around the $C_3—C_4$ bond was obtained by calculating the fully optimized geometry as a function of fixed values of the dihedral angle, $\tau = HC_4C_3C_2$. The absolute minimum of $V(\tau)$ corresponds to the *n*-butyl geometry shown in Figure 2.

Energies relative to those of the corresponding isolated reactants and including thermal corrections are given in Table III for reaction (1) for all alkanes with one to four carbon atoms and for the abstraction of either a primary, a secondary, or a tertiary hydrogen atom. Reactions involving each one of these types were grouped so that trends in activation energies and reaction energies can be clearly observed. The PMP2 absolute values of the activation energies differ by a factor of more than 2 from the experimental values recommended in ref. [5], which is not surprising because these reactions are expected to occur, to a large extent, by tunneling. In addition, part of the difference

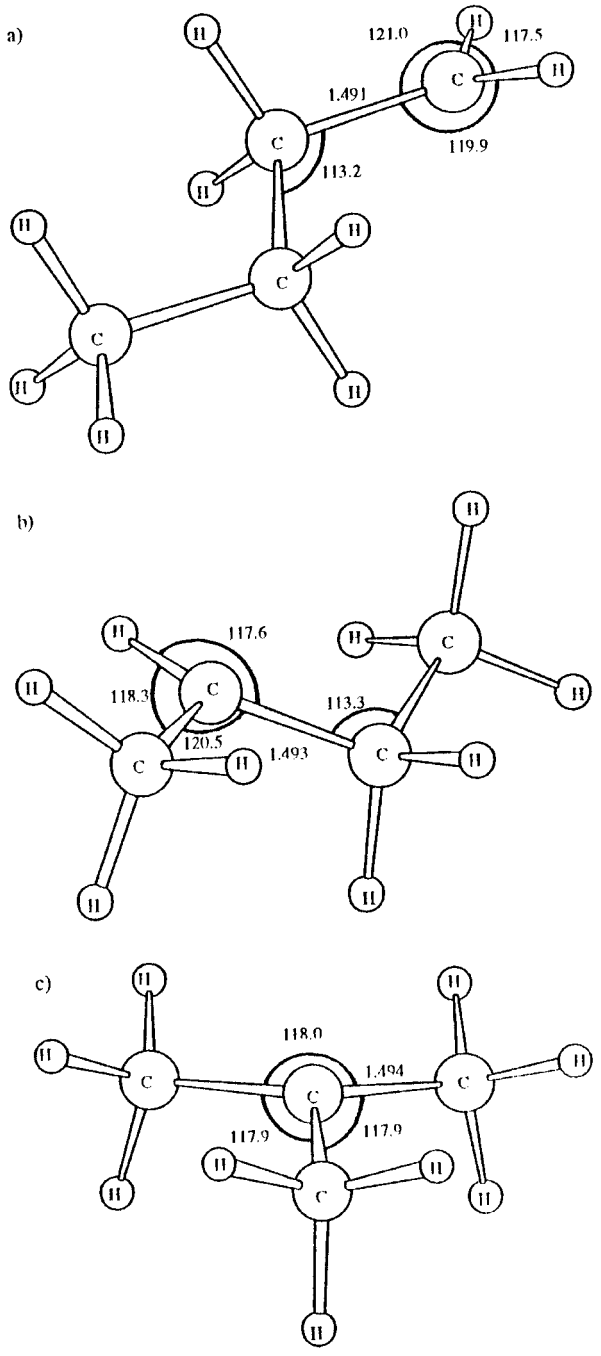

FIGURE 2. Optimized geometries of C_4 alkyl radicals (R·).

should, of course, be attributed to the limitations of the method employed in the calculation (limited basis set, neglect of triple and quadruple interactions, etc.). Very similar calculated activation energies were obtained for all primary hydrogen abstractions (about 4.6 kcal for propane, butane, and isobutane, and somewhat larger values for ethane and methane) and for secondary hydrogens (3.85 for propane, 3.19 for butane). Also, the well-known trend in going from primary to tertiary hydrogen abstraction is obeyed and a 2.41 value was obtained for the tertiary hydrogen in isobutane.

The above results suggest the possibility of performing some sort of scaling of the *ab initio* results. In fact, if one plots the values of the activation energies for the preferred channel of each alkane versus the experimental activation energies of Donahue et al.,[5] one finds an almost linear plot with a correlation coefficient of 0.9990 (Fig. 3). From this plot, the following relationship is established:

$$E_{\text{exp}} = -0.64062 + 0.49369 E_{\text{calc}}. \qquad (9)$$

The 0.494 scaling factor roughly agrees with the estimate of Melissas and Truhlar[11] of a one-half effective decrease in the barrier due to the tunnel effect. For the primary hydrogen abstraction in propane, butane, and isobutane, which have very similar calculated activation energies of about 4.6 kcal, eq. (9) yields a scaled activation energy of 1.6 kcal (Table III).

When the B3LYP energies were used, the same trends were observed. Except for methane, all the activation energies were found to be much too low, being, in fact, negative except for methane. However, the trends were the same as those obtained with PMP2 and a linear correlation, analogous to eq. (9), was obtained between the B3LYP energies and the experimental results, obeying the equation

$$E_{\text{exp}} = 2.98239 + 0.49057 E_{\text{calc}} \qquad (10)$$

with a 0.9995 correlation coefficient. The scaling factor of 0.49057 is remarkably close to the one in eq. (9).

The scaling employed here is, of course, much simpler than the one used by Hu et al.,[13] although both do scale the activation energies to the experimental values. In the SAC method, the basis set is modified to reproduce the experimental energies of reaction for the two half-reactions involved: $RH \rightarrow R + H$ and $H + OH \rightarrow H_2O$. In addition, because the calculated rate constants are found to be consistently lower than the experimental values, a final adjustment to the simulation method is performed by scaling the barrier heights by a factor of 0.85. The classical barrier heights reported in ref. 13 for methane, ethane, propane, and isopropane are included in Table III.

TABLE III.
Activation Energies and Reaction Energies (kcal / mol) for Reaction (1) for Alkanes with One to Four Atoms.

System	Type	E_a (PMP2)	E_a (DFT)	E_a[a]	E_a exp[b]	Δe_{298} (PMP2)[c]	ΔE_{298} DFT	ΔH_{298} exp[d]	ΔH_{298} exp[e]
	Primary H								
Methane		7.76	0.90	6-7	3.4[f]	−11.39		−14.12	−14.38
Ethane		5.47	−1.89	4.0	2.084	−14.09		−18.70	−21.39
Propane		4.66	−2.69	3.2	1.64[g]	−14.17	−12.57	−19.70	−21.39
Butane		4.58	−2.75		1.60[g]	−13.39	−11.83	−21.30	
Isobutane		4.64	−2.60		1.63[g]	−13.03	−11.58	−21.20	
	Secondary H								
Propane		3.85	−3.65	2.2	1.232	−16.34	−15.95	−23.00	−24.39
Butane		3.19	−4.22		0.912	−15.92	−15.66	−24.80	−24.39
	Tertiary H								
Isobutane		2.41	−4.94		0.514	−17.92	−18.86	−26.50	−27.39

Results are grouped according to which type of hydrogen is abstracted. Two sets of experimental values for ΔH_{298} are given. DFT, density functional theory.
[a]Reference 13.
[b]Reference 5.
[c]There is no change in the number of moles in reaction (1), so $\Delta E_{298} = \Delta H_{298}$.
[d]Reference 30.
[e]Reference 32.
[f]Reference 11: Davis, D. D.; Fischer, S.; and Schiff, R. J Chem Phys 1976, 82, 409.
[g]Estimated value, using eq. (9).

Looking at the reaction energies, the PMP2 calculated values for primary hydrogen abstraction were found to be about −13.5 kcal, about −16.0 for secondary hydrogens, and about −18.0 for tertiary hydrogens. Within each group, differences were relatively small. With B3LYP, we found about −12.0 kcal/mol for primary hydrogens and −15.7 and −18.8 kcal/mol for secondary and tertiary hydrogens, respectively. It is interesting to note that the available experimental results for the corresponding reaction enthalpies differ widely among themselves (Table III). Our results agree better with Baulch et al.'s,[33] not in absolute values, but in the sense that, for all primary hydrogen abstractions (except methane), they are very similar, as are the secondary ones. Instead, Cohen and Westberg's experimental results[34] show an increase in ΔH_{298} within the same group as the size of the molecule increases. We did not observe this trend.

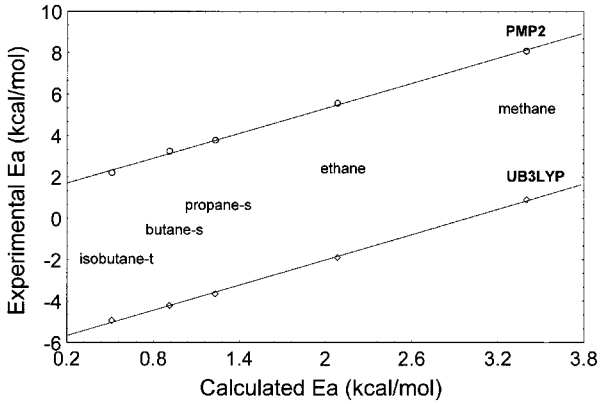

FIGURE 3. A correlation between calculated and experimental[5] activation energies for the OH-alkane hydrogen abstraction reaction.

$R\cdot + O_2$ REACTION

The transition states for the formation of the alkyl peroxyl radicals, whether primary, secondary, or tertiary, present very similar structures with the oxygen molecule lying approximately parallel to a C—C, one oxygen atom interacting with a C atom and the other interacting with a neighboring H atom from either a methyl or a methylene group. The loose five-membered cycles are represented in Figure 4 for propyl, butyl, and isobutyl. As in the case of the abstraction reaction, it is observed that, when going from a primary to a secondary and to a tertiary C···O bond, the transition state appears earlier in the reaction path. The C···O bond is 2.08 Å for all primary additions 2.12–2.13 Å for secondary additions, and 2.18 Å for tertiary additions. In the case of the addition to a secondary carbon of the butyl radical, the other oxygen could, in principle, interact either with a

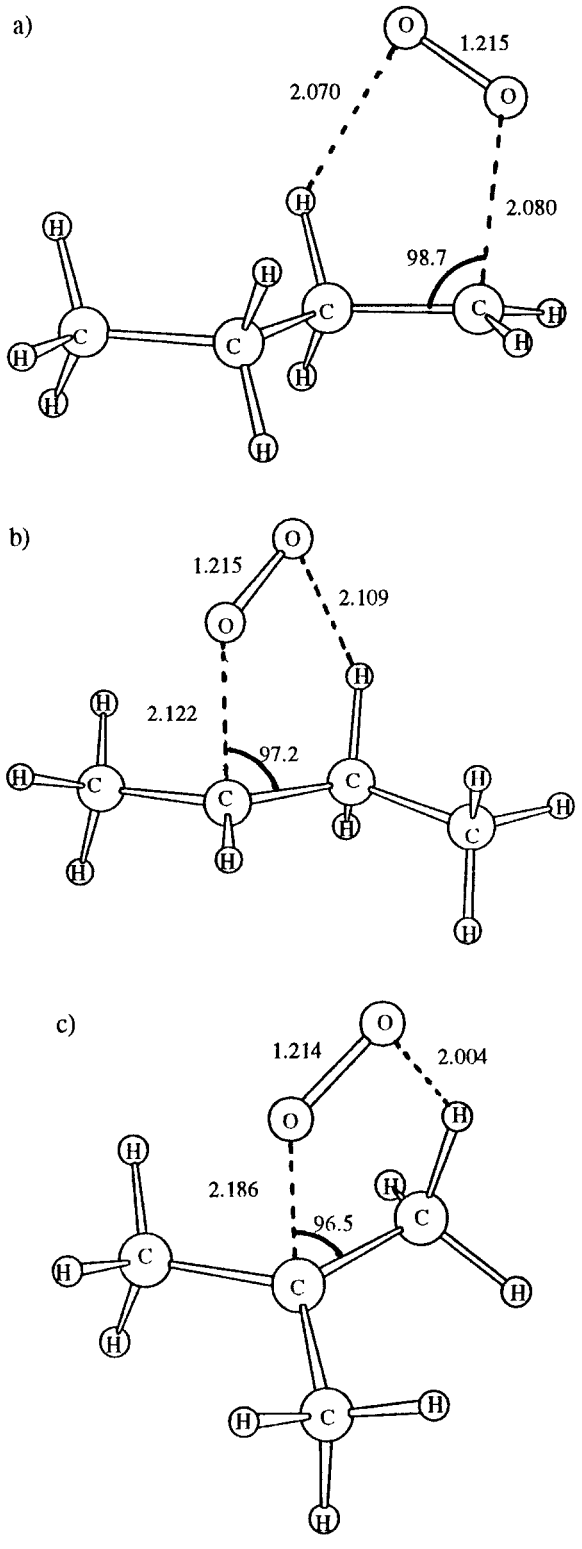

FIGURE 4. Optimized geometries of the transition states (TS2) for the O_2-alkyl radical addition reaction. The TS2 for addition to (a) a primary and (b) a secondary carbon atom of the butyl radical are shown. (c) The TS2 for a tertiary carbon atom from isobutyl is represented.

methyl or with a methylene hydrogen atom. The latter is observed in the preferred conformer.

The optimized structures of the peroxyl radicals are given in Figure 5. Again, close similarities are observed among peroxyls in which the O_2 molecule is attached to the same kind of carbon atom. For primary peroxyls, the O_2 moiety lies above and approximately parallel to the plane of the carbon atoms and in a gauche position with respect to the carbon chain. The external oxygen atom is almost equidistant from carbons 1 and 3. The most stable conformers are similar in shape to the ethylperoxyl radical described in ref. 28. For the secondary and tertiary peroxyls, the O—O bond lies on a line approximately bisecting the C–C–C angle. Some geometrical parameters of the peroxyls are indicated in Figure 5. The geometries of the peroxyl radicals were also optimized with the B3LYP method for comparison. Small differences were observed in the lengths and angles between the two methods. They are indicated in Figure 5 in parentheses.

Charges and spin densities on all atoms were obtained by a Mulliken population analysis using the HF, MP2, and B3LYP electron density. The most significant results are given in Table IV. The results obtained with the MP2 and the B3LYP electron densities are very different from those obtained with the HF density (also indicated in Table IV) and lead to quite different conclusions. In previous work on the structure and properties of several peroxyls,[17,27,35] it was concluded that a large negative charge was always concentrated on the inner oxygen atom while most of the spin density was localized on the outer oxygen atom. The MP2 and the B3LYP densities instead distribute the negative charge almost evenly between both oxygen atoms and locate the unpaired electron at about 0.67 on the outer oxygen atom and 0.33 on the inner one.

The activation energies and reaction energies for reaction (2) calculated with respect to the corresponding $R\cdot + O_2$ are given in Table V for C_1–C_4 alkanes. All activation energies except methane's were found to be negative. For methane there is no possibility of forming a cycle to stabilize the TS2 transition state, which explains why the activation energy is rather large and positive. PMP2 values for primary alkyls are close to -1 kcal/mol, values for secondary alkyls are about -3.5 kcal/mol, and the largest value of -4.9 kcal/mol corresponds to the tertiary isobutyl radical. B3LYP activation energies for primary alkyls are considerably lower at about -8.0 kcal/mol. For secondary and

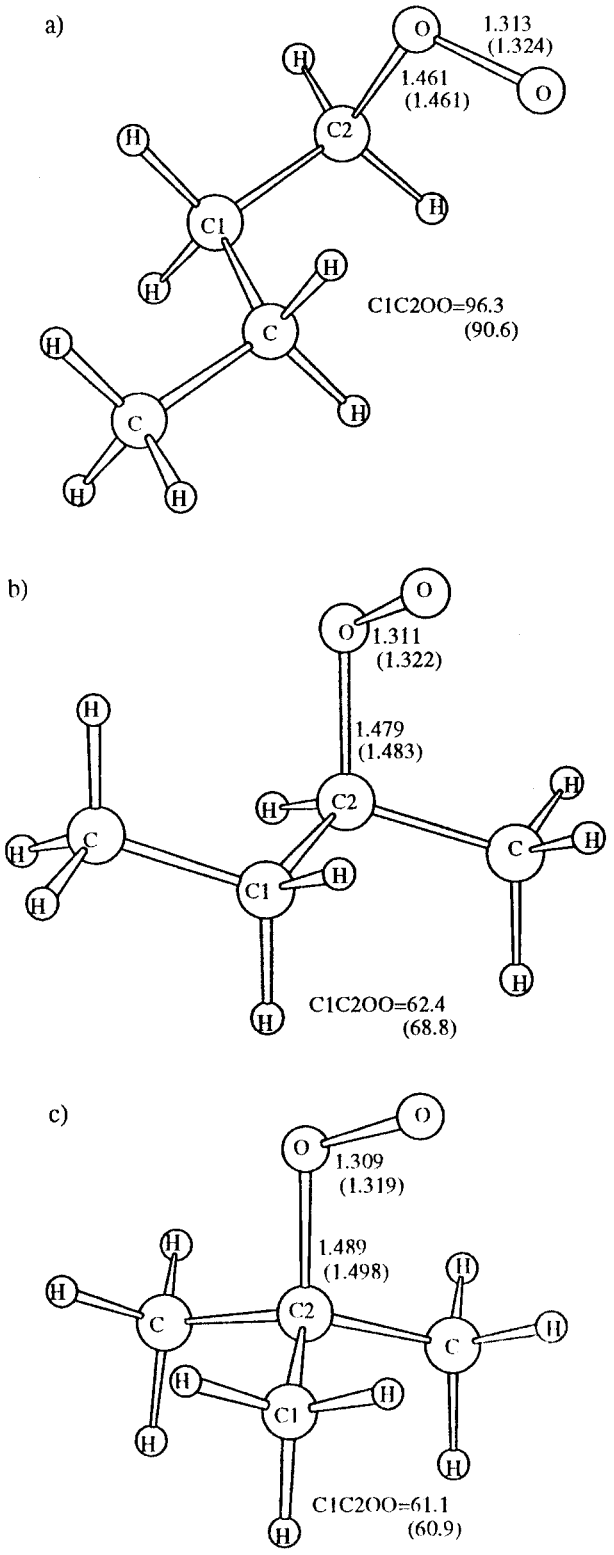

FIGURE 5. Optimized geometries of C_4 peroxyl radicals ($RO_2^{\cdot}$). The values in parentheses were obtained with the density functional method using the B3LYP functional.

tertiary alkyls very similar results were obtained at about 9.4 kcal/mol.

According to the experimental rate constants in Table I, all primary alkyl radicals indeed react with oxygen at rates of about 7.5×10^{-12} cm^{-3} $molecule^{-1}$ s^{-1}, except isobutyl (2-methyl-1-propyl), which has a much smaller rate on the same order as methane's. Our calculated activation energy for this compound, however, is quite close to those of the other primary alkyl peroxyls, which would imply that the preexponential factor should be considerably smaller in this case. This does not seem to be justified. We notice, however, that the value of the rate constant for 2-methyl-1-propyl in Table I was obtained by authors[36] different than the rest,[37,38] so the conditions and methods of the experiments may not have been the same. Also, 2-butyl and 2-propyl present very similar calculated activation energies but quite different experimental rate constants. However, the measured rate for 2-propyl is reported with a very large uncertainty ($+11 \times 10^{-12}$, -5.5×10^{-12}).[37]

Consideration of the energy of the products (the peroxyl radicals) again shows very close values among those involving addition to the same type of carbon and a clear increase in stability as the number of substituent groups on the radical carbon atom increases. These results are in agreement with the reported experimental values. The latter, however, are scarce, because heats of formation of some of the primary alkyl radicals are missing.[33] Using the theoretical results, it is possible to predict that the heat of reaction for the addition of O_2 to 1-propyl, 1-butyl, and 2-methyl-1-propyl should all be approximately equal to -35.0 kcal, the value for the ethyl radical.

Conclusions

We report calculations on two successive reactions involving radical-molecule processes that are the initial reactions in the tropospheric oxidation of alkanes. The reactions of propane, butane, and isobutane with the OH radical and with O_2 were studied by *ab initio* molecular orbital techniques. Structures and properties were obtained after full optimization at the MP2/6-31G** level for all reactants, transition states, and products. Some of the corresponding results for methane and ethane were also calculated and are included in our analysis. Energies, charges, and spin densities were obtained with the PMP2 and the B3LYP methods.

TABLE IV.
Typical Charges and Spin Densities of Peroxyls ($RO_2^{\cdot}$) Obtained by Mulliken Analysis Performed Using Electron Densities Calculated by Different Methods.

R·	Property	UHF	UMP2	B3LYP
Primary				
	Charge on terminal oxygen	−0.08	−0.16	−0.17
	Charge on internal oxygen	−0.33	−0.19	−0.17
	Spin on terminal oxygen	0.91	0.68	0.70
	Spin on internal oxygen	0.10	0.33	0.30
Secondary				
	Charge on terminal oxygen	−0.08	−0.17	−0.17
	Charge on internal oxygen	−0.33	−0.19	−0.18
	Spin on terminal oxygen	0.90	0.67	0.69
	Spin on internal oxygen	0.10	0.34	0.30
Tertiary				
	Charge on terminal oxygen	−0.08	−0.16	−0.17
	Charge on internal oxygen	−0.35	−0.20	−0.19
	Spin on terminal oxygen	0.90	0.67	0.69
	Spin on internal oxygen	0.10	0.34	0.30

The alkyl radicals are named according to the kind of carbon atom to which the O_2 is attached.

Emphasis was placed on the differences between the reactions involving the OH attack on either primary, secondary, or tertiary hydrogen atoms.

Remarkable similarities were observed in the structures and the energy differences among different alkanes when the same kind of atom was involved. In fact, local minima was detected during the geometry optimization by comparing the structures and relative energies of the system under consideration with those of other systems of the same group. Although with the two methods employed the absolute values for the energy differences were always considerably smaller than the experimental results (which, however, are reported with large margins of error), the trends are so clear that scaling factors may be applied and the values obtained could conceivably be used to evaluate the experimental results. A warning should be made, however. Table III shows that the theoretical energy differences vary over a range only about one-half to one-third as wide as the corresponding experimental range. This systematic er-

TABLE V.
Activation Energies and Reaction Energies (kcal / mol) for Reaction (2) for Alkanes with One to Four C Atoms.

System	Type	E_a (PMP2)	E_a (DFT)	E_a exp	ΔE_{298} (PMP2)[a]	ΔS_{298} (DFT)	ΔH_{298} exp[b]
	Primary H						
Methane		6.15			−15.86		−32.4
Ethane		−0.84		−5.06[c]	−19.56		−35.2
Propane		−0.50	−8.02		−19.25	−30.87	
Butane		−1.48	−8.79		−19.72	−31.75	
Isobutane		−0.86	−8.18		−20.26	−31.75	
	Secondary H						
Propane		−3.35	−9.52		−21.89	−31.67	−38.25
Butane		−3.78	−9.40		−22.60	−31.75	−38.54
	Tertiary H						
Isobutane		−4.86	−9.35		−24.01	−31.38	

Results are grouped according to the type of alkyl radical, whether primary, secondary, or tertiary.
[a]For reaction (2), $\Delta E_{298} \approx \Delta H_{298} + 0.6$.
[b]Reference 21.
[c]Reference 36.

ror may mean that the geometric variations are similarly underestimated.[39]

The model proposed by Singleton and Cvetanovic[20] to account for observed negative activation energies in the limit of high pressure was used and negative activation energies were obtained, which also present very clear similarities when the same kind of carbon atom is involved in the peroxyl formation.

Finally, in view of the clear trends obtained in the calculations, we suggest that they can be used to choose among different experimental results, to detect possible anomalies, and to approximately predict unknown results for heats of reaction and for rate constants. As stressed by Donahue et al.,[40] these trends could be further confirmed by investigating similar reactions involving a homologous radical series with the same manifold of molecules.

Acknowledgments

The authors gratefully acknowledge the financial support from the Instituto Mexicano del Petróleo through program FIES-95-97-VI and the computer time on the Silicon Graphics Origin 2000 at the Universidad Nacional Autónoma de México (UNAM).

References

1. Finlayson–Pitts, B. J.; Pitts, N. Atmospheric Chemistry: Fundamentals and Experimental Techniques; Wiley-Interscience: New York, 1986.
2. Blake, D. R.; Rowland, F. S. Science 1995, 269, 953.
3. Atkinson, R. J Phys Chem Ref Data 1997, 26, 215.
4. (a) Atkinson, R. Chem Rev 1985, 85, 69; (b) Atkinson, R. Atmos Environ 1990, 24A, 1 (c) Atkinson, R.; Baulch, D. L.; Cox, R. A.; Hampson, R. F., Jr.; Ker, J. A.; Troe, J. J Phys Chem Ref Data 1989, 18, 881.
5. Donahue, N. M.; Anderson, J. G.; Demerjian, K. L. J Phys Chem 1998, 102, 3121.
6. Bowman, F. M.; Seinfeld, J. H. J Geophys Res 1994, 99, 5309.
7. Calvert, J. G.; Madronich, S. J Geophys Res 1987, 92, 2211.
8. Cohen, N. Int J Chem Kinet 1982, 14, 1339.
9. Cohen, N. Int J Chem Kinet 1991, 16, 469.
10. Atkinson, R.; Carter, W. L. P.; Aschmann, S. M.; Winer, A. M.; Pitts, J. N. Int J Chem Kinet 1984, 23, 297.
11. Melissas, V. S.; Truhlar, D. G. J Chem Phys 1993, 99, 1013.
12. Melissas, V. S.; Truhlar, D. G. J Phys Chem 1994, 98, 875.
13. Hu, W. P.; Rossi, I.; Corchado, J. C.; Truhlar, G. C. J Phys Chem 1997, 101, 6913.
14. Gonzalez–Lafont, A.; Truong, T. N.; Truhlar, D. G. J Chem Phys 1991, 95, 8875.
15. Truong, T. N.; Truhlar, D. G. J Chem Phys 1990, 93, 1761.
16. Sekusak, S.; Gusten, H.; Sablijc, A. J Chem Phys 1995, 102, 7504.
17. García–Cruz, I.; Uc, V. H.; Vivier–Bunge, A.; Smeyers, Y. G. In Computers, Chemistry, and Chemical Engineering, Proceedings of the 3rd UNAM-Cray Supercomputing Conference; Cisneros, G.; Cogordan, J. A.; Castro, M.; Wang, C., Eds.; World Scientific: Singapore, 1997; p 168.
18. Gordon, M. S.; Truhlar, D. G. J Am Chem Soc 1986, 108, 5412.
19. Dobis, O.; Benson, S. W. J Am Chem Soc 1993, 115, 8798.
20. Singleton, D. L.; Cvetanovic, R. J. J Am Chem Soc 1976, 98, 6812.
21. Diaz–Acosta, I.; Alvarez–Idaboy, J. R.; Vivier–Bunge, A. Int J Chem Kinet 1999, 31, 29.
22. Alvarez–Idaboy, J. R.; Diaz–Acosta, I.; Vivier–Bunge, A. J Comp Chem 1998, 19, 811.
23. Lightfoot, P. D.; Cox, R. A.; Crowley, J. N.; Destriau, M.; Hayman, G. D.; Jenkin, M. E.; Moortgat, G. K.; Zabel, F. Atmos Environ 1992, 26A, 1805.
24. Jafri, J. A.; Phillips, D. H. J Am Chem Soc 1990, 112, 2586.
25. Quelch, G. E.; Gallo, M. M.; Schaefer, H. F., III J Am Chem Soc 1992, 114, 8239.
26. Quelch, G. E.; Gallo, M. M.; Shen, M.; Xie, Y.; Schaefer, H. F., III; Moncrieff, D. J Am Chem Soc 1994, 116, 4958.
27. Boyd, S. L; Boyd, R. J.; Barclay, R. C. J Am Chem Soc 1990, 112, 5724.
28. Ignatyev, I. S.; Xie, Y.; Allen, W. D.; Schaefer, H. F., III J Chem Phys 1997, 107, 141.
29. Becke, A. D. J Chem Phys 1993, 98, 5648.
30. Frisch, M. J.; Trucks, G. W.; Schlegel, H. B.; Gill, P. M. W.; Johnson, B. G.; Robb, M. A.; Cheeseman, J. R.; Keith, T. A.; Petersson, G. A.; Montgomery, J. A.; Raghavachari, K.; Al-Laham, M. A.; Zakrzewski, V. G.; Ortiz, J. V.; Foresman, J. B.; Cioslowski, J.; Stefanov, B. B.; Nanayakkara, A.; Challacombe, M.; Peng, C. Y.; Ayala, P. Y.; Chen, W.; Wong, M. W.; Andres, J. L.; Replogle, E. S.; Gomperts, R.; Martin, R. L.; Fox, D. J.; Binkley, J. S.; Defrees, D. J.; Baker, J.; Stewart, J. P.; Head–Gordon, M.; Gonzalez, C.; Pople, J. A. Gaussian 94; Gaussian, Inc.: Pittsburgh, PA, 1995.
31. Dorigo, A. E.; Houk, K. N. J Org Chem 1988, 53, 1650.
32. Alvarez–Idaboy, J. R.; Eriksson, L. A.; Lunell, S. J Phys Chem 1993, 97, 12743.
33. Baulch, D. L.; Bowers, M.; Malcolm, D. G.; Tuckerman, R. T. J Phys Chem Ref Data 1986, 15, 465.
34. Cohen, N.; Westberg, K. R. J Phys Chem Ref Data 1983, 12, 531.
35. Uc, V. H.; García–Cruz, I.; Smeyers, Y. G.; Vivier–Bunge, A. Fol Chim Theor Lat 1994, XXII, 161.
36. Wu, D.; Bayes, K. D. Int J Chem Kinet 1986, 18, 547.
37. Atkinson, R.; Baulch, D. L.; Cox, R. A.; Hampson, Jr., R. F.; Kerr, J. A.; Rossi, M. J.; Troe, J. J Phys Chem Ref Data 1997, 26.
38. Lenhardt, T. M.; McDade, C. E.; Bayes, K. D. J Chem Phys 1980, 72, 304.
39. We thank an anonymous referee for pointing out this fact.
40. Donahue, N. M.; Clarke, J. S.; Anderson, J. G. J Phys Chem 1998, 102, 3923.